ChemComm

COMMUNICATION

View Article Online
View Journal | View Issue

Cite this: *Chem. Commun.*, 2018, **54**, 2436

Received 15th December 2017,
Accepted 7th February 2018

DOI: 10.1039/c7cc09619d

rsc.li/chemcomm

Spatially resolved coding of λ-orthogonal hydrogels by laser lithography†

Rhiannon R. Batchelor,[a] Eva Blasco,[b] Kilian N. R. Wuest,[b] Hongxu Lu,[a] Martin Wegener,[cd] Christopher Barner-Kowollik*[be] and Martina H. Stenzel*[a]

A λ-orthogonal reaction system is introduced, where visible light induced radical thiol–ene and UV light induced NITEC (Nitrile-Imine mediated Tetrazole–Ene Conjugation) ligations are consecutively employed to fabricate and functionalize PEG-based hydrogels. The fluorescent pyrazoline cycloadducts from the NITEC reaction are exploited to visualize the written structures within the hydrogels as well as to attach RGD containing functional groups to promote spatially resolved cell attachment on the hydrogel surface.

Surface patterning on different length scales is of critical interest in various research fields, including optics, electronic and tissue engineering.[1] Potential applications for macroscopic and microscopic structured materials include LEDs, photonic crystals and surfaces for complex cell arrays. Multi-scale assemblies on surfaces with features of different sizes and surface chemistries are typically prepared by a two-step process combining bottom-up and top-down approaches. Photolithography and molding, both top-down techniques, are the most commonly followed avenues, as features with high precisions over wide length scales can be created. While the generated features may entail multiple dimensions, the introduction of surface active groups requires switching to different techniques such as dip-pen lithography.[2] A system where the scaffold and surface structures and functionalities can be written into the material using light without the need for hybrid preparation techniques can therefore facilitate the design of functional polymer surfaces. Such a wavelength-selective system is of particular interest for the design of hydrogels where bioactive groups are carefully placed into the material with high spatial and temporal control.[3–6]

The use of wavelength-selective reactions in a one-pot system was recently pioneered by some of us[7] and termed 'λ-orthogonal ligation chemistry', defined as the preference of one reaction over another by using a specific wavelength. Our earlier study introduced a λ-orthogonal ligation strategy based on *o*-methyl benzaldehyde and tetrazole driven chemistry. This wavelength selective system has been used to create different polymer architectures from star polymers[8] to micro-scale polymer networks.[9] Light-induced reactions have recently seen a renaissance in soft matter materials design. The photo-induced radical thiol–ene reaction,[10–12] as well as the tetrazine–ene[13] and tetrazole–ene[14] (NITEC) reactions are examples of light induced crosslinking reactions utilised for the formation of poly(ethylene glycol) (PEG)-based hydrogel networks. Continuing the click chemistry paradigm[15,16] in hydrogel synthesis, the utilisation of multiple orthogonal reactions to both fabricate and functionalise the hydrogel is a powerful concept. The combination of light-driven reactions with photopatterning using masks of desired shapes is an important method used to imprint patterns into the gel, as the desired click reaction only occurs where the light is applied. For example, photopatterning with UV initiated thiol–ene reactions with a norbornene functionalised hyaluronic hydrogel provided different moduli in the photopatterned areas.[5] A further study showed the photopatterning of a thiol–yne fabricated gel with excess alkyne groups that were further functionalised by azide in the CuAAc chemistry.[3] Deforest and Anseth[6] however, took orthogonal reactions to the next level, showing that a thiol–ene reaction and an *o*-nitrobenzyl ether degradation crosslinker can be activated selectively based on the employed wavelength. The hydrogel was fabricated by a thermal SpAAc reaction wherein the peptide crosslinker contained vinyl groups and a UV degradable *o*-nitrobenzyl ether linkage. Herein, the concept of λ-orthogonality is exploited for cell patterning on hydrogels.

[a] *Centre for Advanced Macromolecular Design, School of Chemistry, University of New South Wales (UNSW), Sydney, Australia. E-mail: m.stenzel@unsw.edu.au*
[b] *Macromolecular Architectures, Institut für Technische Chemie und Polymerchemie, Karlsruhe Institute of Technology (KIT), Engesserstr. 18, 76131 Karlsruhe, Germany. E-mail: Christopher.barner-kowollik@kit.edu*
[c] *Institute of Applied Physics, Karlsruhe Institute of Technology (KIT), Wolfgang-Gaede-Straße 1, 76128 Karlsruhe, Germany*
[d] *Institute of Nanotechnology, Karlsruhe Institute of Technology (KIT), Hermann-von-Helmholtz-Platz 1, 76344 Eggenstein-Leopoldshafen, Germany*
[e] *School of Chemistry, Physics and Mechanical Engineering, Queensland University of Technology (QUT), 2 George Street, Brisbane, QLD 4000, Australia. E-mail: christopher.barnerkowollik@qut.edu.au*

† Electronic supplementary information (ESI) available: Experimental details. See DOI: 10.1039/c7cc09619d

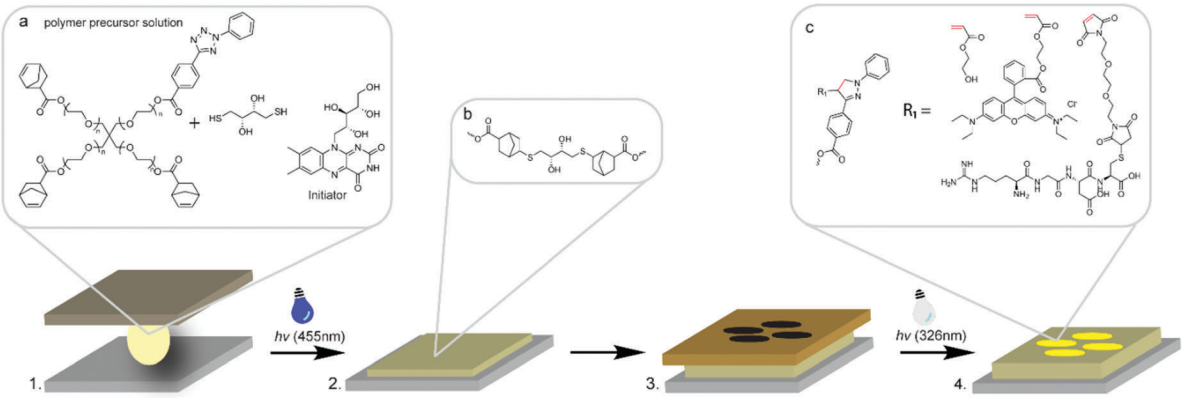

Scheme 1 General procedure for the fabrication and functionalisation of the PEG based hydrogels. (1) Precursor solution placed between a methacrylate functional glass slide and PDMS cover. (2) Irradiated under blue light to obtain the crosslinked gel. (3) Gel swollen with acrylate solution and photomask placed on top. (4) Irradiated under UV light to obtain patterned sections. (a) Hydrogel precursor solution. 1 : 1 equivalent of DTT and norbornene moieties. (b) Crosslinks consist of a double thioether linkage. (c) Chemistry of the photopatterned areas.

Two wavelength selective reactions, the thiol–ene reaction and nitrile-imine tetrazole–ene coupling (NITEC) are employed, one in the formation of the scaffold using a functionalized 4-arm PEG macromer and the other as a tethering point within the scaffold for further functionalization, to anchor functional groups that can encourage cell attachment (Scheme 1). The thiol–ene reaction has been used extensively for preparing PEG based hydrogels and is known to be rapid and cytocompatible, while the profluorescent product of the NITEC reaction provides a self-reporting spectroscopic handle indicating successful ligation events. Thus, this platform technology is suitable to create hydrogel surfaces with potentially a multitude of functional groups.

First, identifying the correct wavelengths at which the thiol–ene and NITEC reactions are selectively activated was imperative, since both tetrazole and thiol can readily react with electron poor and strained alkenes (the norbornene in this system).[17–19] Key to establishing λ-orthogonality in our system is selecting the optimum photoinitiator for the thiol–ene reaction such that this coupling will proceed without interference from the competing NITEC reaction. Often lithium phenyl-2,4,6-trimethylbenzoylphosphinate (LAP) is employed at a UV irradiation wavelength of 365 nm.[20] However, riboflavin is utilised in the current system, exhibiting a visible absorption maximum at 440 nm. Upon irradiation with a commercially available LED lamp at a similar wavelength, riboflavin can be selectively excited to initiate the radical thiol–ene reaction[11] prior to the NITEC reaction wherein the tetrazole is only activated in the UV region.

Prior to proceeding with the formation of the hydrogel, it was critical to demonstrate the λ-orthogonality of the system by employing small molecules as a model system. A poly(ethylene glycol) monomethyl ether chain (M_n = 5000 Da) was capped with 4-(2-phenyl-2*H*-tetrazol-5-yl) benzoic acid (tetrazole) and employed in a one pot system also containing excess 5-norbornene-2-methanol, 2-mercaptoethanol and the blue light initiator riboflavin in D_2O/MeOD-d_4 medium. An LED lamp with an absorption maximum at 455 nm and fluorescent lamp Arimed B6 with a maximum wavelength at 326 nm was employed for the activation of riboflavin and the tetrazole, respectively (Fig. S1, ESI†). The reaction mixture was initially irradiated with blue light (27 mW cm^{-2}) for 1 h and subsequently exposed to UV light (1.58 mW cm^{-2}) for 7 h. A sample was taken before and after each irradiation step for analysis by ^{1}H NMR spectroscopy (Fig. 1). After irradiation under blue light, the triplet resonance assigned to the α-protons on 2-mercaptoethanol at 2.5 ppm disappeared, indicating the thiol–ene reaction had occurred. The signal corresponding to the α-protons on the thioether is not evident in the spectrum due to overlap with the PEG and norbornene resonances. Importantly, the tetrazole moiety remains intact as evidenced by the unaffected peaks at 7–8 ppm corresponding to the aromatic protons on the tetrazole moiety. After irradiation under UV light, the aromatic tetrazole resonances disappeared, whereas five new downfield resonances corresponding to the pyrazoline adduct, indicate the successful NITEC reaction between the tetrazole and the norbornene.

Once the wavelength selectivity of the above described reactions was established, PEG based polymers were utilised for the preparation of hydrogels due to their ease of functionalisation, high solubility in water and biocompatibility.[20–24] A four-arm polyethylene glycol (PEG) star (M_n = 20 000 Da) was reacted with carboxylic acid functional biphenyl tetrazole and carboxylic acid functional norbornene derivatives in two sequential *N*-(3-dimethylaminopropyl)-*N*′-ethylcarbodiimide hydrochloride (EDC) mediated coupling reactions to obtain a non-toxic (Fig. S2, ESI†), end group functionalised PEG (0.7 : 3; tetrazole/norbornene). The multifunctional PEG macromer was reacted with a stoichiometric amount of dithiothreitol in the presence of 0.3 mM riboflavin at a macromer content of 10 wt% at 455 nm to form the hydrogel network through the radical thiol–ene reaction between norbornene moieties and the dithiol crosslinker (Scheme 1). The network gelation was determined by oscillatory rheometry and found to be 32 s (Fig. S3, ESI†). Removal of riboflavin by immersion in water provides a clear gel allowing a qualitative indication that the colourless tetrazole moieties

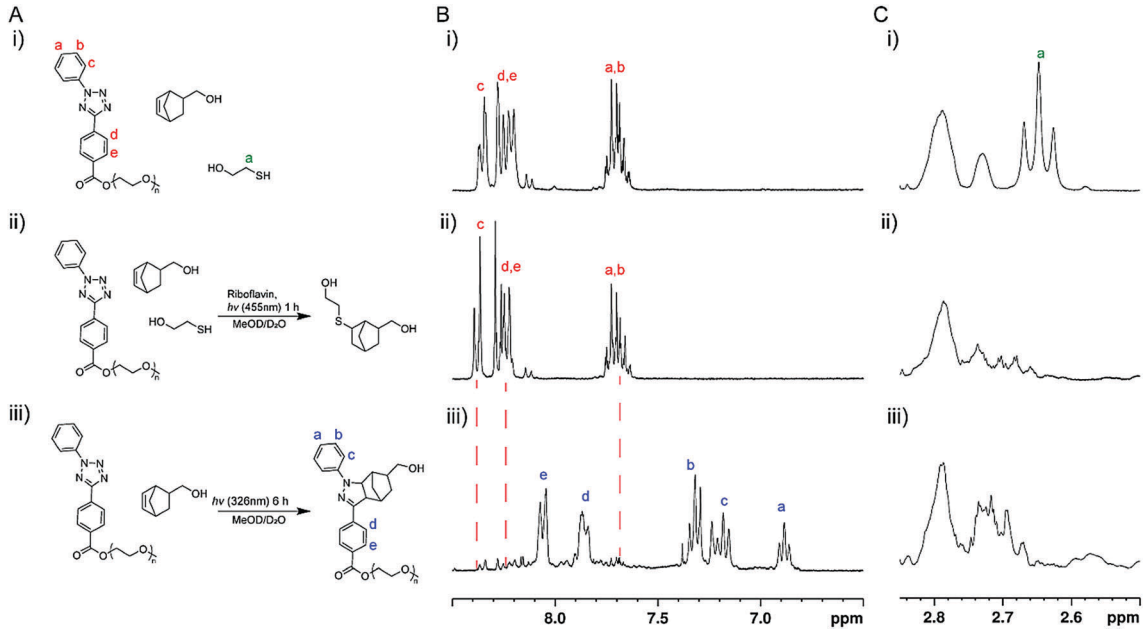

Fig. 1 Small molecule reactions for establishing λ-orthogonality. (A) (i) PEG-Tet, mercaptoethanol and 5-norbornene-2-methanol before irradiation. (ii) After blue irradiation, (iii) after UV irradiation. (B) ^{1}H NMR spectra of the aromatic region. (C) ^{1}H NMR spectra of the mercaptoethanol resonances region.

remain unreacted, as the pyrazoline product of the NITEC reaction absorbs at 330–450 nm and appears yellow to the naked eye (Fig. S4, ESI†). ^{1}H NMR spectra of the crosslinked gel also show the tetrazole remains intact while the norbornene has reacted, indicating crosslinking *via* the thiol–ene coupling (Fig. S5 and S6, ESI†). After the established network formation, the gels were swollen with an aqueous solution of either 2-hydroxy ethyl acrylate (HEA) or rhodamine B ethyl acrylate (RhBEA). The visible light absorbance at 445 nm of the pyrazoline was exploited to probe the kinetics of the NITEC reaction in this system (Fig. S7, ESI†) and it was found that the NITEC ligation ceased after 35 min.

By irradiating through a photomask, the NITEC reaction was confined to specific locations within the gel. One of the most appealing features of the NITEC reaction is the strong fluorescence of the reaction product, *i.e.*, pyrazoline. The characteristic fluorescence of the pyrazoline has been exploited before in cellular imaging[25,26] and imaging of NITEC written structures.[9,27] Here, we use it to provide a visualisation technique when lithography techniques are applied, where in other systems fluorescent tagging is required for visualisation. In our system, a photomask was applied to the gels and irradiated for 1 h under UV light. After dialysis to remove the unreacted acrylates, the gels were imaged under UV light (for the HEA system) using a standard UV lamp or confocal fluorescence microscopy, or visible light for the dye RhBEA (Fig. S8, ESI†). Fig. 3 displays the size range of photopatterning achieved through standard lithography techniques from several centimetres for the KIT and UNSW logos down to 20 μm. Critically, two-photon direct laser writing (DLW) (λ = 530 nm) has been employed to prepare 2D micropatterns. Initially, dose tests consisting of lines written at powers between 0 and 5 mW and at different height to prove the suitability of writing inside the hydrogel were performed (Fig. S9, ESI†). It was found that the NITEC reaction was triggered employing relatively low laser power (below 1 mW) at the writing speed of 100 μm s^{-1}. Subsequently, 1 mW and 100 μm s^{-1} were set as writing conditions and a 2D micropattern consisting of a 10 μm checkerboard pattern was created inside the hydrogel. As expected, the micropatterns exhibited a strong fluorescence indicating a successful NITEC functionalization (Fig. 2d). The advantage of using DLW instead of conventional lithographic techniques relies on the possibility of patterning arbitrary features without the necessity of using a mask and with high resolution.

To demonstrate the potential of λ-orthogonal hydrogel systems for cell cultures, a cell binding motif was attached in a spatially resolved pattern. The peptide sequence RGD is an integrin binding motif and promotes cell adhesion. The RGD sequence was functionalised with a bismaleimide linker through a base catalysed Michael thiol–ene addition to the RGDC cysteine residue (ESI†). The RGDC-maleimide was diffused into the hydrogel over a few hours and irradiated through a photomask for 2 h. After being immersed in water for 12 h to remove residual RGDC-maleimide, the gel was sterilised by immersion in ethanol. After immersion in water, human dermal fibroblasts (NHDF) were seeded onto the hydrogel surface and cultured over 24 h. As shown in Fig. 3, the cells only attach to the irradiated sections of the hydrogel surface, *i.e.* where the RGD was covalently attached *via* the NITEC reaction. No attachment was seen in the control sample.

In summary, we introduce λ-orthogonality between a visible light-induced radical thiol–ene and UV light-induced NITEC ligation, consecutively employed to fabricate and functionalise PEG-based hydrogels. Standard lithographic techniques as well as DLW were employed to functionalise hydrogel scaffolds in a spatially resolved fashion. The fluorescent pyrazoline cycloadducts

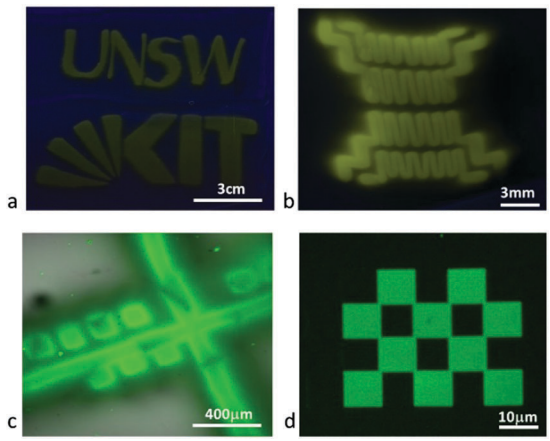

Fig. 2 Photopatterned hydrogels using 2-hydroxyethyl acrylate as the alkene. Photopattern imaged under UV lamp (a) and (b). Confocal fluorescence image of a photopatterned hydrogel (c). (d) Confocal fluorescence image of checkerboard pattern written by direct laser writing (DLW) at the glass hydrogel interface.

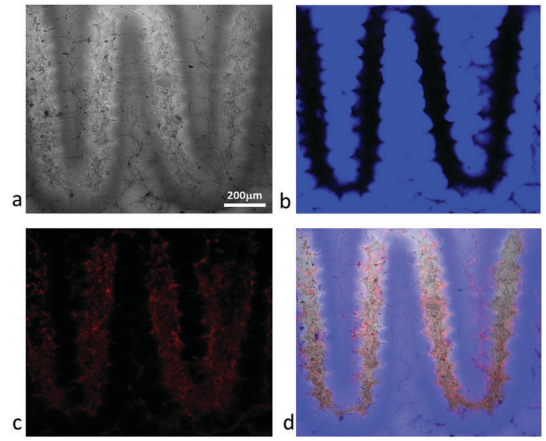

Fig. 3 Surface adhesion of NHDF cells. (a) DIC image of NHDF cells after 24 h incubation on the hydrogel surface. (b) Fluorescence confocal image of the photopatterned section of the gel (photopatterned areas appear black). (c) Fluorescence confocal image of NHDF cells stained with propidium iodide. (d) Merged image of (b) and (c).

from the NITEC reaction were exploited to visualize the functionalized structures within the hydrogels. In addition, the versatility and biocompatibility of the introduced λ-orthogonal approach was demonstrated by the spatially resolved surface patterning of NHDF cells on the hydrogel. We submit that our herein pioneered approach for spatially resolved hydrogel coding constitutes a versatile platform for potential mechanical and chemical manipulation of hydrogels.

C. B.-K. acknowledges funding from the Queensland University of Technology (QUT) as well as the Karlsruhe Institute of Technology (KIT) in the context of the STN and BIFTM programs. C. B.-K. additionally acknowledges the Australian Research Council (ARC) for key funding in the context of a Laureate Fellowship enabling his photochemical research program. The authors acknowledge the NMR facility of the Mark Wainwright Analytical Centre, G. Kwandou and A/Prof. P. Spicer (UNSW) for their assistance with rheological measurements and Patrick Müller (KIT) for his assistance with DLW. RB would like to thank UNSW for the Australian Government Research Training Program Scholarship.

Conflicts of interest

There are no conflicts to declare.

Notes and references

1 Z. Nie and E. Kumacheva, *Nat. Mater.*, 2008, **7**, 277–290.
2 X. Zhou, F. Boey, F. Huo, L. Huang and H. Zhang, *Small*, 2011, **7**, 2273–2289.
3 B. J. Adzima, Y. Tao, C. J. Kloxin, C. A. DeForest, K. S. Anseth and C. N. Bowman, *Nat. Chem.*, 2011, **3**, 256–259.
4 X. Wang, C. Yan, K. Ye, Y. He, Z. Li and J. Ding, *Biomaterials*, 2013, **34**, 2865–2874.
5 W. M. Gramlich, I. L. Kim and J. A. Burdick, *Biomaterials*, 2013, **34**, 9803–9811.
6 C. A. DeForest and K. S. Anseth, *Nat. Chem.*, 2011, **3**, 925–931.
7 K. Hiltebrandt, T. Pauloehrl, J. P. Blinco, K. Linkert, H. G. Börner and C. Barner-Kowollik, *Angew. Chem., Int. Ed.*, 2015, **54**, 2838–2843.
8 K. Hiltebrandt, M. Kaupp, E. Molle, J. P. Menzel, J. P. Blinco and C. Barner-Kowollik, *Chem. Commun.*, 2016, **52**, 9426–9429.
9 M. Kaupp, K. Hiltebrandt, V. Trouillet, P. Mueller, A. S. Quick, M. Wegener and C. Barner-Kowollik, *Chem. Commun.*, 2016, **52**, 1975–1978.
10 B. D. Fairbanks, M. P. Schwartz, A. E. Halevi, C. R. Nuttelman, C. N. Bowman and K. S. Anseth, *Adv. Mater.*, 2009, **21**, 5005–5010.
11 R. R. Batchelor, G. Kwandou, P. T. Spicer and M. H. Stenzel, *Polym. Chem.*, 2017, **8**, 980–984.
12 N. Gupta, B. F. Lin, L. M. Campos, M. D. Dimitriou, S. T. Hikita, N. D. Treat, M. V. Tirrell, D. O. Clegg, E. J. Kramer and C. J. Hawker, *Nat. Chem.*, 2010, **2**, 138–145.
13 D. L. Alge, M. A. Azagarsamy, D. F. Donohue and K. S. Anseth, *Biomacromolecules*, 2013, **14**, 949–953.
14 Y. Fan, C. Deng, R. Cheng, F. Meng and Z. Zhong, *Biomacromolecules*, 2013, **14**, 2814–2821.
15 H. C. Kolb, M. G. Finn and K. B. Sharpless, *Angew. Chem., Int. Ed.*, 2001, **40**, 2004–2021.
16 C. Barner-Kowollik, F. E. Du Prez, P. Espeel, C. J. Hawker, T. Junkers, H. Schlaad and W. Van Camp, *Angew. Chem., Int. Ed.*, 2011, **50**, 60–62.
17 A. B. Lowe, *Polym. Chem.*, 2014, **5**, 4820–4870.
18 E. Blasco, Y. Sugawara, P. Lederhose, J. P. Blinco, A.-M. Kelterer and C. Barner-Kowollik, *ChemPhotoChem*, 2017, **1**, 159–163.
19 Y. Wang, C. I. Rivera Vera and Q. Lin, *Org. Lett.*, 2007, **9**, 4155–4158.
20 S. B. Anderson, C.-C. Lin, D. V. Kuntzler and K. S. Anseth, *Biomaterials*, 2011, **32**, 3564–3574.
21 J. A. Benton, B. D. Fairbanks and K. S. Anseth, *Biomaterials*, 2009, **30**, 6593–6603.
22 S. J. Bryant, R. J. Bender, K. L. Durand and K. S. Anseth, *Biotechnol. Bioeng.*, 2004, **86**, 747–755.
23 P. M. Kharkar, M. S. Rehmann, K. M. Skeens, E. Maverakis and A. M. Kloxin, *ACS Biomater. Sci. Eng.*, 2016, **2**, 165–179.
24 G. N. Grover, J. Lam, T. H. Nguyen, T. Segura and H. D. Maynard, *Biomacromolecules*, 2012, **13**, 3013–3017.
25 W. Song, Y. Wang, J. Qu, M. M. Madden and Q. Lin, *Angew. Chem.*, 2008, **120**, 2874–2877.
26 M. M. Madden, C. I. Rivera Vera, W. Song and Q. Lin, *Chem. Commun.*, 2009, 5588–5590.
27 M. Dietrich, G. Delaittre, J. P. Blinco, A. J. Inglis, M. Bruns and C. Barner-Kowollik, *Adv. Funct. Mater.*, 2012, **22**, 304–312.